

We are IntechOpen, the world's leading publisher of Open Access books Built by scientists, for scientists

6,900

Open access books available

186,000

International authors and editors

200M

Downloads

Our authors are among the

154

Countries delivered to

TOP 1%

most cited scientists

12.2%

Contributors from top 500 universities



WEB OF SCIENCE™

Selection of our books indexed in the Book Citation Index
in Web of Science™ Core Collection (BKCI)

Interested in publishing with us?
Contact book.department@intechopen.com

Numbers displayed above are based on latest data collected.
For more information visit www.intechopen.com



Temperature Sensing Characteristics of Tapered Doped Fiber Amplifiers

*Rafael Sanchez-Lara, Lelio de la Cruz-May,
José Luis Vazquez-Avila,
Daniel Enrique Ceballos-Herrera and
José Alfredo Alvarez-Chavez*

Abstract

We numerically analyze the temperature response of tapered doped fiber amplifiers and discuss their feasibility to be used as a sensing element in temperature fiber sensors. In particular, we consider Ytterbium (Yb) and Thulium (Tm) rare earths in the tapered doped fiber designs. We have modified the coupled propagation equations for the pump and signal radiations in order to include different taper structures and introduce the temperature dependence of the absorption and emission cross-sections of Yb and Tm ions. It was found that the temperature sensitivity of the amplified signal in Tm-doped fiber amplifiers is one order of magnitude higher than this obtained with Yb-doped fibers. Additionally, in all doped fibers, the temperature sensitivity of the signal radiation is higher for low pump powers in a co-propagating pump scheme, and it highly depends on the longitudinal shape of the taper used. Finally, for both Yb- and Tm-doped fibers, the temperature sensitivity can be increased if we use doped fiber lengths shorter than 1 m and pump powers lower than 300 mW. This study provides valuable information for the development of tapered fiber amplifiers doped with other rare earths and novel designs for doped fiber temperature sensors.

Keywords: ytterbium, thulium, taper, doped fiber, sensors

1. Introduction

Non-invasive sensors for temperature and strain measurements in explosive environments and with immunity to electromagnetic interference are constantly required. In this context, optical fibers have become a key piece to develop temperature sensors in such hazardous applications. As an example of these applications, we can mention petroleum pipeline monitoring and hydraulic fracturing evaluations [1, 2]. Consequently, many efforts have been made to improve the performance of fiber optic temperature sensors based on different principles and designs.

The development of temperature and strain fiber sensors for environmental measurements where immunity to electromagnetic interference and high personal safety are required has been studied with great interest until today. This fact has allowed the development of a large number of fiber optic temperature sensors based in different principles and designs; among them, we can distinguish two principal groups which are based in doped [3–10] and un-doped fibers [11–17]. In the first group, we have sensors that use the temperature dependence of the fluorescence lifetime and involve techniques as the fluorescence intensity ratio. In these sensors, the key parameter is the temperature dependence of the absorption and emission cross-sections of the pump and signal in the doped fiber amplifier [18–22]. On the other hand, the second group of temperature sensors are based on un-doped fibers, and these use principally interference techniques. As examples, we can mention sensors based on Fabry-Perot interferometers, fiber Bragg gratings, long-period gratings, optical fiber couplers, and tapered fibers [11–17]. The key parameter in these sensors is the temperature dependence of the dielectric material that modifies the modal behavior of the signal that propagates in the un-doped fiber. It consequently changes the interferometer condition and generates a power variation at the end of the fiber device. Currently, several works have been performed to improve the sensitivity of these temperature sensors employing a combination of these sensing techniques in doped and un-doped fibers, respectively. Additionally, these combinations have allowed discerning between simultaneous strain and temperature measurements [3–6]. In this context, the gradual progress to develop improved temperature fiber sensors requires the necessity to explore continuously novel configurations based on the sensing techniques described above. At this point, one interesting proposal is to consider the use of a tapered fiber, amply used as a temperature fiber sensor [11–17], inscribed simultaneously in a doped fiber amplifier, which poses an additional temperature response caused by its cross-sections [3–10, 18–21]. At this respect, only the efficiency of pump absorption in tapered doped fiber lasers has been studied [23, 24], but a detailed analysis of its temperature response has not been performed. Therefore, in this chapter, we present an analysis of the temperature sensing characteristics of a tapered Yb- and Tm-doped fiber amplifier, and we explore its feasibility to be used as sensing element in temperature fiber sensors. In the present analysis, we study the thermal response of the tapered doped fiber with different tapered fiber structures and pump schemes to find an optimized design for temperature sensing.

2. Numerical simulation

We start our analysis considering first a tapered fiber section formed in a single-mode step index fiber surrounded by air. This scheme has been extensively studied in un-doped fibers showing that no changes of the transmitted power by temperature are obtained when only air is considered as surrounding media [11–14]. These modifications on the transmitted power are reached when a thermochromic material surrounds the tapered fiber section. However, this situation is not considered in our study because our principal interest is to analyze the transmitted power variations caused by the temperature response of the amplified spontaneous emission in the tapered doped core.

Once air is considered as the surrounding media, we proceed to analyze the mode field expression of the fundamental core mode within the tapered fiber. The mode field expression is an important parameter in doped fiber amplifiers because it determines the core mode fraction of the pump and signal, which affects the power conversion in the doped core [23–28]. In this study, Gaussian shapes for the pump

and signal fundamental core modes were considered. Thus, we can write the transverse intensity pattern using a Gaussian envelope approximation given by [29]:

$$f_{p,s}(r) = \frac{1}{\pi\Omega^2} e^{-r/\Omega^2} \quad (1)$$

where subscripts p and s refer to pump and signal radiations and Ω is determined by the characteristic of the fiber: the refractive indexes and radius of the core and cladding, respectively. The multiplying factor in Eq. (1) is chosen to normalize $f(r)$ as follows:

$$2\pi \int f_{p,s}(r) dr = 1 \quad (2)$$

For a step index fiber, Ω is approximately given by [29]:

$$\Omega = aJ_0(U) \frac{V K_1(W)}{U K_2(W)} \quad (3)$$

where a is the core radius and $U = a\sqrt{k^2 n_1^2 - \beta^2}$, $W = a\sqrt{\beta^2 - k^2 n_1^2}$, $V = ka\sqrt{n_1^2 - n_2^2}$, $k = \frac{2\pi}{\lambda}$, n_1 and n_2 are the refractive indices of the active core and cladding, respectively, and β is the propagation constant of the pump or signal mode. For a given V , the value of W can be obtained using the empirical relationship

$$W = 1.1428V - 0.996, \quad (4)$$

It is valid only for step index fibers. In this way, according to the pump and signal wavelengths, one can obtain the respective values of U , W , and V using the numerical aperture (NA) of the fiber where

$$NA = \sqrt{n_1^2 - n_2^2}, \quad (5)$$

and subsequently the parameter Ω . This procedure is accurate for $1.5 < V < 2.5$.

Now, we analyze the thermal effects on the tapered doped fiber considering the changes of the absorption and emission cross-section with temperature. Previous works in un-tapered fibers have reported changes in population of the energy levels in Yb-doped glasses, and the broadening of the homogeneous linewidth as temperature is increased [18–21]. It results in modifications of the absorption and emission cross-sections for the signal and pump radiations. These effects may vary for each individual doped fiber due to the different glass composition, concentration of dopants and co-dopants, and the degree of structural disorder on the glass network used in different active fibers. In particular, we study the impact of variations on the cross-sections due to temperature in tapered doped fiber amplifiers. Without loss of generality, we use the absorption and emission cross-section changes with temperature reported in [18], which is a representative of several Yb-doped fibers. These changes are expressed in the following equations:

$$\sigma(T) = \sigma(20^\circ\text{C}) + \frac{d\sigma}{dT} \quad (6)$$

$$\frac{d\sigma_{abs}^{1064nm}}{dT} = 7.78 * 10^{-29} \frac{m^2}{^\circ K} \quad (7)$$

$$\frac{d\sigma_{em}^{1064nm}}{dT} = -2.44 * 10^{-28} \frac{m^2}{^\circ K} \quad (8)$$

$$\frac{d\sigma_{abs}^{976nm}}{dT} = \frac{d\sigma_{em}^{976nm}}{dT} = -1.63 * 10^{-27} \frac{m^2}{^\circ K} \quad (9)$$

where σ_{abs}^{1064nm} and σ_{em}^{1064nm} are the absorption and emission cross-sections for the signal wavelength and σ_{abs}^{976nm} and σ_{em}^{976nm} are the absorption and emission cross-sections for the pump wavelength, respectively.

In order to model a temperature-dependent tapered Yb-doped fiber amplifier, we numerically analyze the following coupled equations:

$$\frac{dI_p(r, z)}{dz} = [\sigma_{em}^p(T)n_2(T) - \sigma_{abs}^p(T)n_1(T)]N_{tot}I_p(r, z) \quad (10)$$

$$\frac{dI_s(r, z)}{dz} = [\sigma_{em}^s(T)n_2(T) - \sigma_{abs}^s(T)n_1(T)]N_{tot}I_s(r, z) \quad (11)$$

where $I_p(r, z)$ and $I_s(r, z)$ are the pump and signal intensities; N_{tot} is the total ytterbium population; $\sigma_{abs}^p, \sigma_{em}^p, \sigma_{abs}^s, \sigma_{em}^s$ are the temperature dependent absorption and emission cross-sections of the pump and signal at 976 nm and 1064 nm, respectively; and $n_1(T), n_2(T)$ are the temperature-dependent upper- and lower-state populations of Yb, which are given at a steady state by the following equations:

$$n_2 = \frac{R_{abs} + W_{abs}}{R_{abs} + R_{em} + W_{abs} + W_{em} + A_{esp}} \quad (12)$$

$$n_1 = 1 - n_2 \quad (13)$$

where $R_{abs} = \sigma_{abs}^p I_p h\nu_p$, $R_{em} = \sigma_{em}^p I_p h\nu_p$, $W_{abs} = \sigma_{abs}^s I_s h\nu_s$, and $W_{em} = \sigma_{em}^s I_s h\nu_s$. In these equations, the ASE generation is not considered, and only effects of the taper and temperature modifications are investigated.

In order to consider the taper effects and the overlap of the pump and signal fundamental mode with the active core, we can use [29]:

$$I_{p,s} = P_{p,s}(z)f_{p,s}(r) \quad (14)$$

where subscripts p and s refer to pump and signal radiations, $P_{p,s}(z)$ are the z -dependent powers at the pump and signal wavelengths, and $f(r)$ is given by Eq. (1). It is clear at this point that the effect of taper and temperature in parameter Ω defined in Eq. (3) directly modifies the evolution of pump and signal intensities described in Eqs. (10) and (11).

If we consider the pump power at any value of z , we have [30]

$$P_{p,s}(z) = \int_0^\infty \int_0^{2\pi} I_{p,s}(r, z) r dr d\phi = 2\pi \int_0^\infty I_{p,s}(r, z) r dr \quad (15)$$

Then,

$$\frac{dP_{p,s}(z)}{dz} = 2\pi \int_0^\infty \frac{dI_{p,s}(r, z)}{dz} r dr \quad (16)$$

Using Eqs. (14) and (16), we can rewrite Eqs. (10) and (11) as follows:

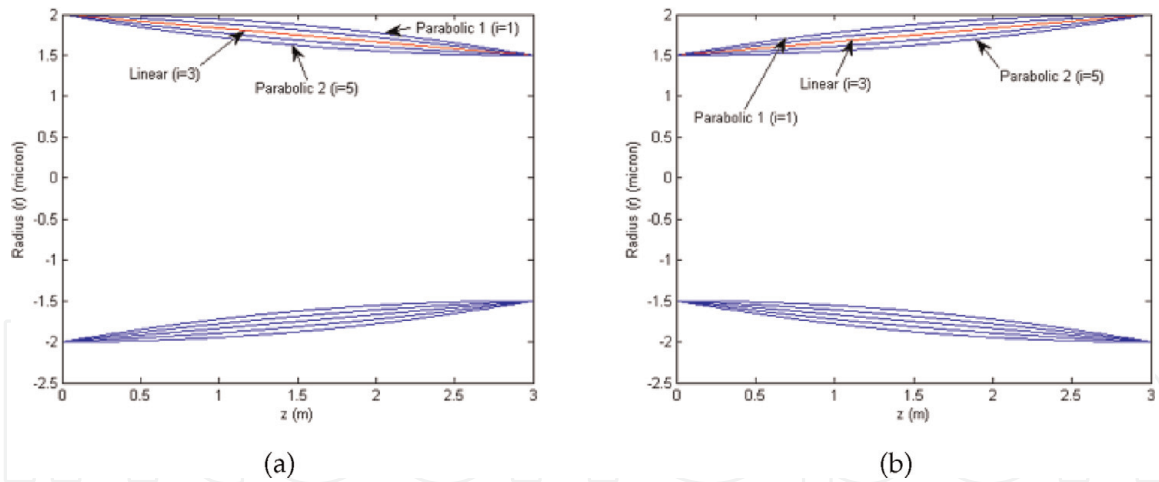


Figure 1. Modeling scheme using tapered Yb-doped amplifiers with different tapered core shapes and with co-propagating single pump at different initial taper ends: (a) pump at the end with wider radius and (b) pump at the end with lower radius.

$$\frac{dP_p(z)}{dz} = 2\pi \int_0^{a(z)} [\sigma_{em}^p(T)n_2(T) - \sigma_{abs}^p(T)n_1(T)] N_{tot} f_p(r) r dr \quad (17)$$

$$\frac{dP_s(z)}{dz} = 2\pi \int_0^{a(z)} [\sigma_{em}^s(T)n_2(T) - \sigma_{abs}^s(T)n_1(T)] N_{tot} f_s(r) r dr \quad (18)$$

On these equations, we assume that the fiber is doped with uniform Yb concentration up to the core radius “a” which depends on z . Besides, it is worth to note that $n_1(T)$ and $n_2(T)$ depend on $f_{p,s}(r)$ due to their relation with I_p and I_s intensities.

Once the temperature-dependent coupled equations are defined, we proceed to model a tapered Yb-doped fiber amplifier with different longitudinal tapered core shapes and different pump schemes [31] as is shown in **Figure 1**.

$$r(z) = \frac{1}{C} (-D - Bz - z^2) \quad (19)$$

$$r(z) = \frac{1}{C} (-D - B(L - z) - (L - z)^2) \quad (20)$$

This model can be applied to a different doped material as the thulium; in this case Eqs. (6) to (9) must be replaced in agreement with absorption and emission cross-section changes with temperature reported in [32–35]. These changes are expressed in the following equations:

$$\sigma_{abs}^{1600nm}(T) = 15.56 \times 10^{-25} - 38 \times 10^{-28} T \quad (21)$$

$$\sigma_{em}^{1600nm}(T) = 1.8 \times 10^{-26} + 1.99 \times 10^{-28} T \quad (22)$$

$$\sigma_{abs}^{1841nm}(T) = -1.96 \times 10^{-26} + 3.53 \times 10^{-28} T \quad (23)$$

$$\sigma_{em}^{1841nm}(T) = 3.75 \times 10^{-25} - 1.57 \times 10^{-29} T \quad (24)$$

3. Results and discussion

As a first step, we analyze the power conversion along the fiber between the pump and signal radiations for the different taper schemes described in 0. In

addition, we consider the following absorption and emission cross-sections for the Yb-doped fiber amplifier at 20 °C: $\sigma_{abs}^p = 1.488 \times 10^{-24} \text{ m}^2$, $\sigma_{em}^p = 1.829 \times 10^{-24} \text{ m}^2$, $\sigma_{abs}^s = 6 \times 10^{-27} \text{ m}^2$, and $\sigma_{em}^s = 3.58 \times 10^{-25} \text{ m}^2$, where the wavelengths 976 and 1064 nm correspond to the pump and signal radiation, respectively. In the numerical simulation, we have fixed the numerical aperture of 0.18 along the tapered fiber, and we change the temperature from 20 to 120 °C. In both taper structures named Taper 1 (**Figure 1a**) and Taper 2 (**Figure 1b**), we employ a pump power of

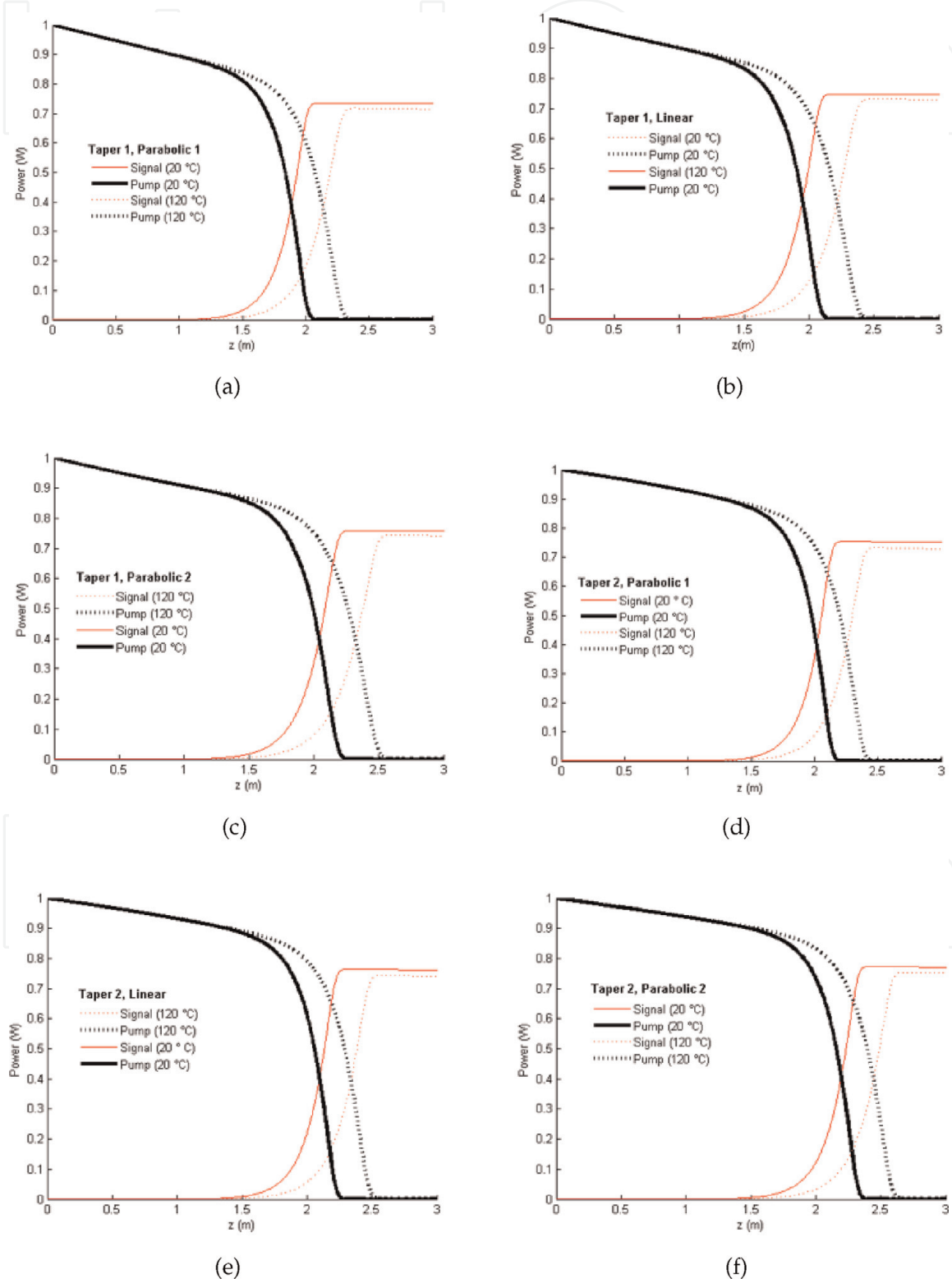


Figure 2.

Modeling of a tapered Yb-doped amplifier. Evolution of the pump and signal radiations at two different temperature; (a), (b) and (c) for the scheme named taper 1 at 1 W of pump power for different tapered core shapes; (d), (e), and (f) for the scheme named taper 2 at 1 W of pump power for different tapered core shapes.

1 W, and the corresponding numerical results are shown in **Figure 2** for each tapered structure. In this figure it is relevant to observe the behavior of the cross-point where the signal and pump conversion occurs, due to the fact that this cross-point shifts to different lengths according to temperature variations. Then, this shift is an indicative of which tapered structure is affected principally by temperature, modifying in this way the Yb-doped fiber amplifier performance. To visualize this temperature response in a better way, we proceed to analyze the amplified signal power at the end of the tapered fiber at 20°C with respect to the signal generated at different temperatures T using the following normalized expression:

$$[P_s(20^\circ\text{C}) - P_s(T)] / P_s(20^\circ\text{C}). \tag{25}$$

We evaluate this equation for each tapered structure given in **Figure 1**. In the calculations we employ a fiber length = 3 m, and a pump power = 1 W. The results are shown in **Figure 3**. According to **Figure 3**, all tapered fiber structures show a high temperature sensitivity for large values of temperature. In addition, we can observe that the tapered fiber structure named Taper 2 is more sensitive to temperature for different tapered shapes. Especially, for the Taper 2 with a parabolic-1 shape, we obtain an improvement of the temperature sensitivity in the fiber amplifier.

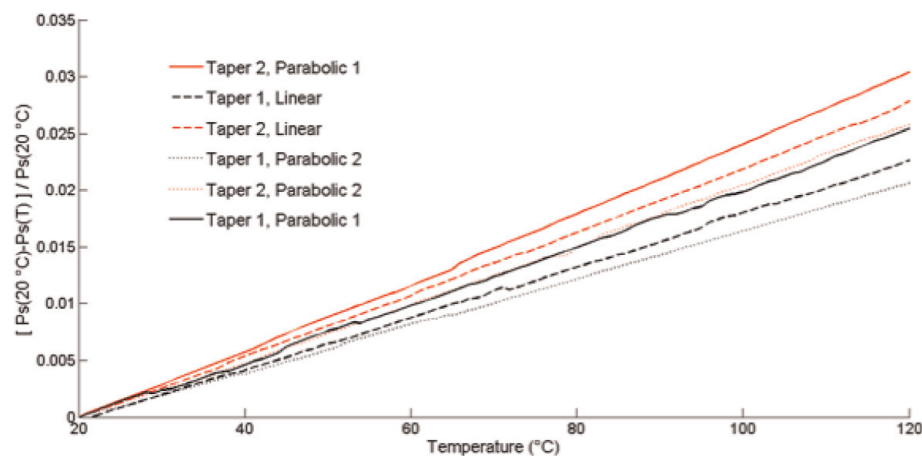


Figure 3.
Efficiency signal conversion for different temperatures at the end of the tapered fiber.

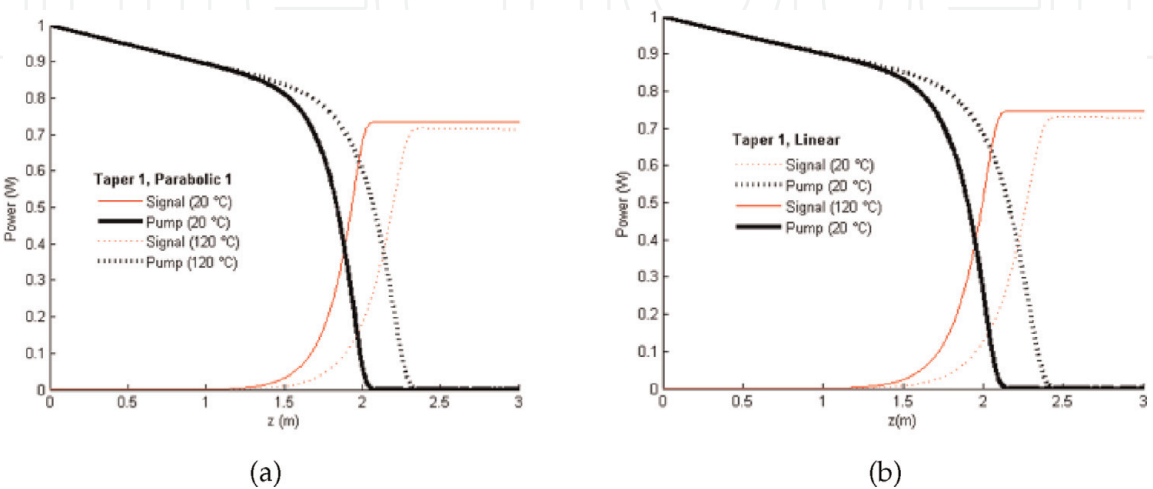


Figure 4.
Temperature behavior of the generated signal for different temperatures $T = 30$ and 120°C at different pump powers: 0.1 – 0.5 W.

Temperature response at different pump powers is shown in **Figure 4**, where temperatures of 30 and 120°C are used. The signal is calculated at the end of the tapered fiber (3 m) according to the scheme of **Figure 1**.

According to **Figure 4**, the temperature sensitivity of the signal radiation for both tapered fiber schemes shown in **Figure 1** is higher as the temperature is increased, and it can be improved if we employ lower pump powers than 1 W, respectively. In particular, this increment on sensitivity highly depends on the taper

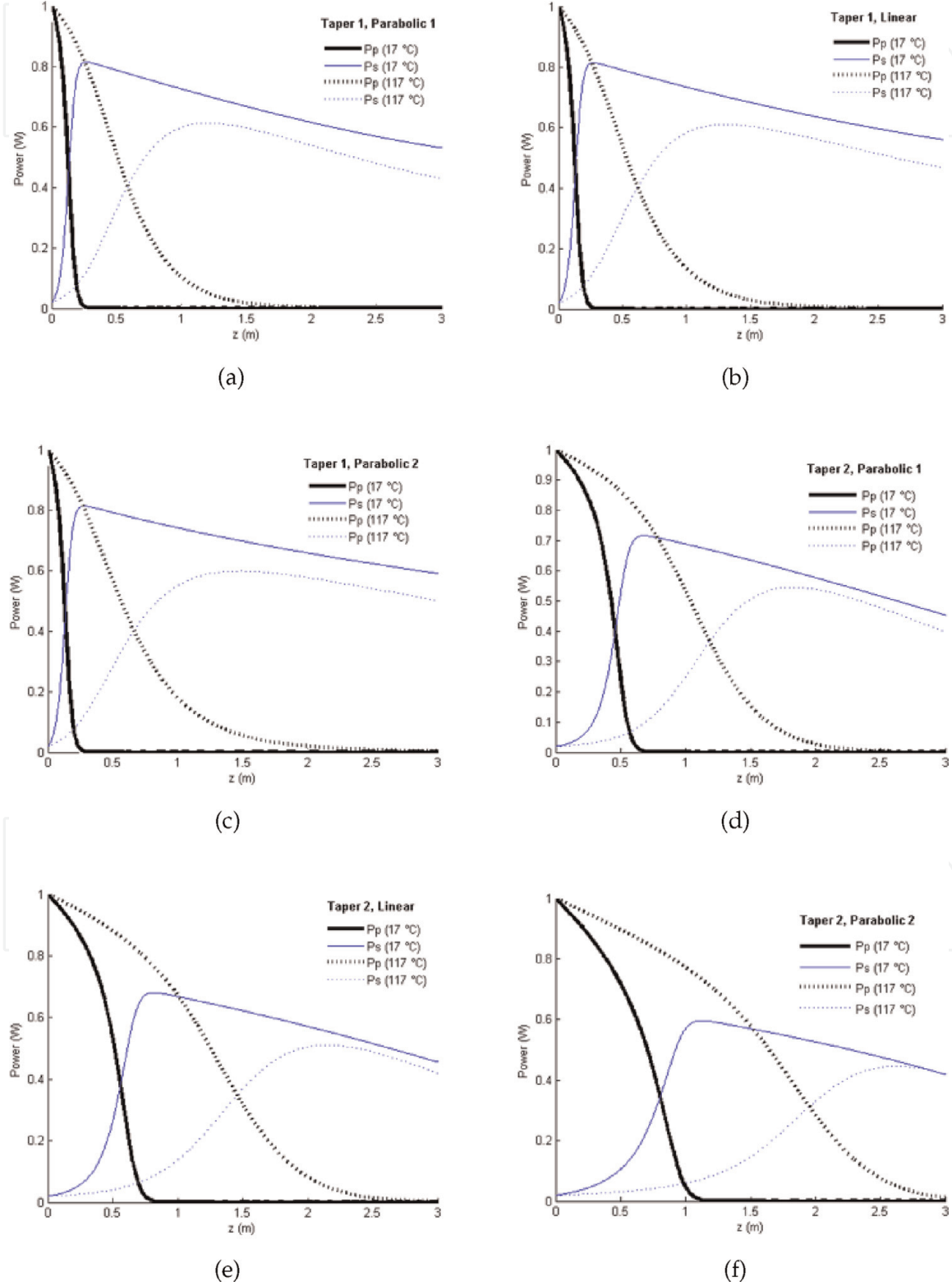


Figure 5. Modeling of a tapered Tm-doped amplifier. Evolution of the pump and signal radiations at two different temperatures,; (a), (b), and (c) for the scheme named taper 1 at 1 W of pump power for different tapered core shapes; (d), (e), and (f) for the scheme named taper 2 at 1 W of pump power for different tapered core shapes.

shape and the pump scheme employed in the amplifier design. Additionally, this temperature sensitivity can change according to the tapered fiber length. In our calculations, the tapered length was 3 m, but other temperature sensitivities can be obtained if we consider tapered fiber length between 2 and 2.5 m, where the cross-point of the signal and pump radiations is located (See **Figure 2**). In this sense, further analysis needs to be performed to optimize the temperature sensitivity using different taper ratios and different taper lengths and modifying the longitudinal shape of the tapered doped fiber amplifier. Similarly, in the case of T_h , we analyze the radiation conversion along the fiber between the pump and signal radiations of the different schemes described in **Figure 1**. The numerical aperture $NA = 0.18$ is considered constant along the taper, and the temperature is changed from 17–117°C. For both schemes shown in **Figure 1**, the co-propagating pump and signal power were set at 1 W and 20 mW, respectively; the corresponding results of the signal conversion for three different temperatures are shown in **Figure 5** for each longitudinal tapered core shape.

According to **Figure 6**, all tapered doped fiber amplifiers show an increasing temperature sensitivity for values starting even at 27°C and up to the maximum temperature of 117°C. The curves for “Taper 2” scheme (all in blue color) showed a saturation at around 87°C, indicating less sensitivity to temperature with respect to “Taper 1” scheme (in black color). However, this behavior could vary if we use other fiber lengths. In this context, the curves shown in **Figure 5** represent a design map that could allow us to choose the taper shape and its corresponding taper length, given by the cross-point in order to improve the temperature sensitivity of the tapered doped fiber amplifier around a specific temperature value.

On the other hand, **Figure 7** shows the temperature response at different pump powers for the two tapered core shapes analyzed in this work, where temperatures of 27 and 117°C are used. The signal is calculated at the end of the tapered fiber (3 m) according to the scheme of **Figure 1**.

According to **Figure 7**, the temperature sensitivity of the tapered doped fiber amplifier grows as the temperature is increased, and it is higher for low values of the pump power. This is an important result to consider for the design of fiber lasers and temperature fiber sensors. Therefore, we can consider that the temperature sensitivity of the signal radiation is higher for low pump powers, and this sensitivity is different for each pump scheme and depends on the taper used. This sensitivity can vary according to the length of the fiber used. For example, these calculations were made at 3 m; however, more sensitivity changes can be obtained at shorter length, as it is shown in **Figure 2**. Additionally, further analysis needs to be

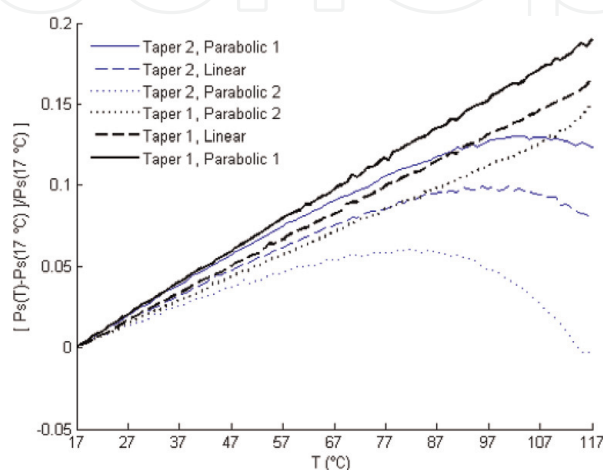


Figure 6.
 Normalized amplified signal for different temperatures at the end of the tapered fiber with $L = 3$ m.

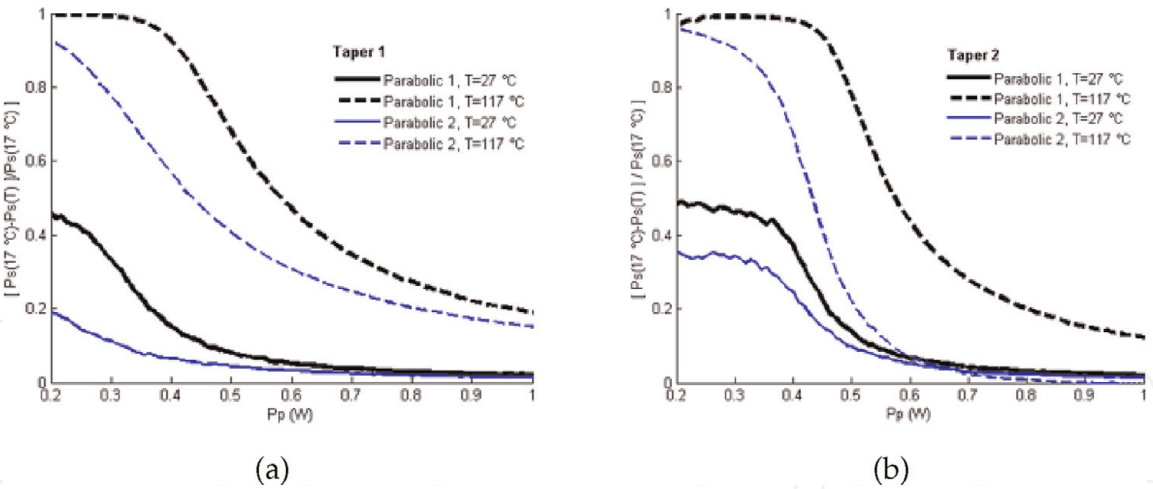


Figure 7. Temperature behavior of the generated signal for temperatures $T = 300$ and 390°K at different pump powers (0.2–1 W): (a) taper 1, parabolic 1 and 2, (b) taper 2, parabolic 1 and 2.

Sensing material	λ pump (nm)	Fluorescence wavelengths (nm)	Temperature range ($^{\circ}\text{C}$)	Sensitivity ($^{\circ}\text{C}^{-1}$)	Reference
Er: silica fiber	800	530/555	23–600	0.013	[10]
Yb: silica fiber	810	910/1030	20–600	0.095	[31]
Nd: silica fiber	807 nm	820–840/895–815	–50–500	0.168	[3]
Er: silica fiber	785	527–537/545–555	21–96	0.006	[8]
Yb: tapered silica fiber	976	1064	15–120	0.005	This work
Tm: tapered silica fiber	1650	1841	17–117	0.009	This work

Table 1. Comparison of the performance of rare-earth-doped fibers and materials as temperature-sensing elements.

performed to optimize the temperature sensitivity using different taper ratios and the longitudinal shape of the tapered doped fiber.

Similar results were obtained as in the case of using an Yb-doped fiber amplifier for temperature sensing. However, although the response follows a similar behavior, the results are different, the evolution of the pump and signal radiation is shifted to shorter lengths along the fiber, the efficiency signal conversion is larger, and the temperature behavior of the generated signal for different temperatures as a function of the pump power shows an increased response for the Tm-doped fiber amplifier. The sensitivity of both tapers can be compared with other kinds of sensor of temperatures using similar techniques as shown in **Table 1**. **Table 1** compares the parameters of the authors' tapered ytterbium- and thulium-doped fiber temperature sensors with existing ones. It can be seen that the sensitivity of the sensors is close to early work on doped silica fibers for intrinsic fiber-optic temperature sensors.

4. Conclusion

We have reported a numerical analysis of the temperature effects in tapered ytterbium and thulium-doped fiber amplifiers in co-propagation mode. We found that the tapering shape and the pump power at the input amplifier modify

significantly its temperature sensitivity. In particular, the temperature sensitivity is higher as the core radius is reduced in the propagation direction (Taper 1 scheme), and it can be maximized if the tapered fiber length is equal to the propagation distance where the cross-point of the power conversion is achieved. On the other hand, the temperature sensitivity can also be incremented if we use lower pump powers at the amplifier input. Then, for temperature sensing applications, it is desirable to work using tapered doped fiber amplifiers in low pump power regimes. Our results can be extrapolated to other doped fibers and are of great interest for the improvement of high-power tapered lasers and the development of temperature fiber laser sensors.

Acknowledgements

The authors gratefully acknowledge UNACAR and the Optical Sciences Group at The University of Twente.

Conflict of interest

The authors declare no conflict of interest.

Author details

Rafael Sanchez-Lara^{1*†}, Lelio de la Cruz-May^{1†}, José Luis Vazquez-Avila^{1†}, Daniel Enrique Ceballos-Herrera^{2†} and José Alfredo Alvarez-Chavez^{3†}

1 Facultad de Ingenieria, Universidad Autonoma del Carmen (UNACAR), Ciudad Del Carmen, Campeche, Mexico


2 Instituto de Ingenieria, Universidad Nacional Autonoma de Mexico (UNAM), Cd. Universitaria, Mexico

3 Optical Sciences Group, University of Twente, Enschede, The Netherlands

*Address all correspondence to: rafaunacar@gmail.com

† These authors contributed equally.

IntechOpen

© 2019 The Author(s). Licensee IntechOpen. This chapter is distributed under the terms of the Creative Commons Attribution License (<http://creativecommons.org/licenses/by/3.0>), which permits unrestricted use, distribution, and reproduction in any medium, provided the original work is properly cited. 

References

- [1] Sukkar K, Mahmood S, Alhuda H, Jabbar N. Temperature sensing for petroleum pipelines monitoring and control using fiber optics. In: 3rd International Scientific Conference New Trends in Information Technology and Communications Applications (NTICT). Baghdad: In Cooperation with IEEE and UOITC; 2017
- [2] Amini S, Kavousi P, Carr TR. Application of fiber-optic temperature data analysis in hydraulic fracturing evaluation: A case study in marcellus shale. In: Unconventional Resources Technology Conference (URTeC'2017). Austin, Texas: Society of Exploration Geophysicists, American Association of Petroleum; 24-26 July 2017. pp. 2105-2115
- [3] Wade S, Baxter G, Collins S, Grattan K, Sun T. Simultaneous strain-temperature measurement using fluorescence from Yb-doped silica fiber. *The Review of Scientific Instruments*. 2000;**71**(6):2267-2269
- [4] Liu T, Fernando G, Zhang Z, Grattan K. Simultaneous strain and temperature measurements in composites using extrinsic Fabry-Perot interferometric and intrinsic rare-earth doped fiber sensors. *Sensors and Actuators, A: Physical*. 2000;**80**(3): 208-215
- [5] Trpkovski S, Wade SA, Collins SF, Baxter GW. Er³⁺:Yb³⁺ doped fibre with embedded FBG for simultaneous measurement of temperature and longitudinal strain. *Measurement Science and Technology*. 2005; **16**(2):488
- [6] Jung J, Nam H, Lee JH, Park N, Lee B. Simultaneous measurement of strain and temperature by use of a single-fiber Bragg grating and an erbium-doped fiber amplifier. *Applied Optics*. 1999;**38**(13):2749-2751
- [7] Wade SA, Collins SF, Baxter GW. Fluorescence intensity ratio technique for optical fiber point temperature sensing. *Journal of Applied Physics*. 2003;**94**(8):4743-4756
- [8] Paez G, Strojnik M. Experimental results of ratio-based erbium-doped-silica temperature sensor. *Optical Engineering*. 2003;**42**(6):1805-1812
- [9] Maurice E, Monnom G, Dussardier B, Saïssy A, Ostrowsky D, Baxter G. Erbium-doped silica fibers for intrinsic fiber-optic temperature sensors. *Applied Optics*. 1995;**34**(34): 8019-8025
- [10] Castrellon-Urbe J, García-Torales G. Remote temperature sensor based on the up-conversion fluorescence power ratio of an erbium-doped silica fiber pumped at 975 nm. *Fiber and Integrated Optics*. 2010;**29**(4):272-283
- [11] Zhu S, Xing JW, Pang FF, Wang TY. Temperature sensor based on a single-mode tapered optical fiber. *Journal of Shanghai University (English Edition)*. 2011;**15**(2):101
- [12] Kim KT, Park KH. Fiber-optic temperature sensor based on single mode fused fiber coupler. *Journal of the Optical Society of Korea*. 2008;**12**(3): 152-156
- [13] Prerana P, Varshney RK, Pal BP, Nagaraju B. High sensitive fiber optic temperature sensor based on a side-polished single-mode fiber coupled to a tapered multimode overlay waveguide. *Journal of the Optical Society of Korea*. 2010;**14**(4):337-341
- [14] Díaz-Herrera N, Navarrete M, Esteban O, González-Cano A. A fibre-optic temperature sensor based on the deposition of a thermochromic material

on an adiabatic taper. *Measurement Science and Technology*. 2003;**15**(2):353

[15] Villatoro J, Monzón-Hernández D, Mejía E. Fabrication and modeling of uniform-waist single-mode tapered optical fiber sensors. *Applied Optics*. 2003;**42**(13):2278-2283

[16] Zhu S, Pang F, Wang T. Single-mode tapered optical fiber for temperature sensor based on multimode interference. In: *Asia Communications and Photonics Conference and Exhibition (ACP'2011)*. Shanghai, China: Optical Society of America; 13-16 November 2011. p. 83112B

[17] Monzón-Hernández D, Mora J, Perez-Millán P, Díez A, Cruz JL, Andrés MV. Temperature sensor based on the power reflected by a Bragg grating in a tapered fiber. *Applied Optics*. 2004;**43**(12):2393-2396

[18] Henry LJ, Shay TM, Hult DW, Rowland KB. Thermal effects in narrow linewidth single and two tone fiber lasers. *Optics Express*. 2011;**19**(7):6164-6176

[19] Vazquez-Zuniga LA, Chung S, Jeong Y. Thermal characteristics of an ytterbium-doped fiber amplifier operating at 1060 and 1080 nm. *Japanese Journal of Applied Physics*. 2010;**49**(2R):022502

[20] Peng X, Dong L. Temperature dependence of ytterbium-doped fiber amplifiers. *JOSA B*. 2008;**25**(1):126-130

[21] Newell T, Peterson P, Gavrielides A, Sharma M. Temperature effects on the emission properties of Yb-doped optical fibers. *Optics Communication*. 2007;**273**(1):256-259

[22] Saito K, Yamamoto R, Kamiya N, Sekiya E, Barua P. Fictive temperature dependences of optical properties in

Yb-doped silica glass. In: *Proceeding of Spie 2008*. San Diego, California, United States: International Society for Optics and Photonics; 10-14 August 2008. p. 69981-J

[23] Filippov V, Chamorovskii Y, Kerttula J, Golant K, Pessa M, Okhotnikov O. Double clad tapered fiber for high power applications. *Optics Express*. 2008;**16**(3):1929-1944

[24] Li L, Lou Q, Zhou J, Dong J, Wei Y, Du S, et al. High power single transverse mode operation of a tapered large-mode-area fiber laser. *Optics Communication*. 2008;**281**(4):655-657

[25] Alvarez-Chavez J, Grudinin A, Nilsson J, Turner P, Clarkson W. Mode selection in high power cladding pumped fibre lasers with tapered section. In: *Technical Digest. Summaries of papers presented at the Conference on Lasers and Electro-Optics (CLEO'99)*. Baltimore, MD, USA: Conference on Lasers and Electro-Optics IEEE; 28-28 May 1999. p. 247-248

[26] Ustimchik V, Nikitov S, Chamorovskii YK. Simulation of radiation generation in an active double-clad optical tapered fiber. *Journal of Communications Technology and Electronics*. 2011;**56**(10):1249

[27] Bagan V, Nikitov S, Chamorovskii YK, Shatrov A. Studying the properties of double-clad active cone optic fibers. *Journal of Communications Technology and Electronics*. 2010;**55**(10):1154-1161

[28] Zhang YJ, Zhong FF, Wang YZ. Top-hat beam Tm³⁺-doped fiber laser using an intracavity abrupt taper. *Laser Physics*. 2011 Jan;**21**(1):215-218. DOI: 10.1134/S1054660X11010245

[29] Ghatak A, Thyagarajan K. *An introduction to fiber optics*. 1st ed. Cambridge: Cambridge University

Press; 1998. p 576. DOI: 10.1017/
CBO9781139174770

[30] Alvarez-Chavez JA, Perez-Sanchez G, Ceballos-Herrera D, Rodriguez-Rodriguez J, Schreiber T. Temperature sensing characteristics of tapered Yb-doped fiber amplifiers. *Optik*. 2013; **124**(22):5818-5821

[31] Sanchez-Lara R, Ceballos-Herrera D, Vazquez-Avila J, de la Cruz-May L, Martinez-Pinon F, Alvarez-Chavez J. Temperature sensing characteristics of tapered Tm³⁺-doped fiber amplifiers. *Laser Physics*. 2017; **27**(8):085108

[32] Turri G, Sudesh V, Richardson M, Bass M, Toncelli A, Tonelli M. Temperature-dependent spectroscopic properties of Tm³⁺ in germanate, silica, and phosphate glasses: A comparative study. *Journal of Applied Physics*. 2008; **103**(9):093104

[33] Sudesh V, Piper J, Goldys E, Seymour R. Growth, characterization, and laser potential of Tm: La₂Be₂O₅. *JOSA B*. 1998; **15**(1):239-246

[34] Agger SD, Povlsen JH. Emission and absorption cross section of thulium doped silica fibers. *Optics Express*. 2006; **14**(1):50-57

[35] Payne SA, Chase L, Smith LK, Kway WL, Krupke WF. Infrared cross-section measurements for crystals doped with Er³⁺, Tm³⁺, and Ho³⁺. *IEEE Journal of Quantum Electronics*. 1992; **28**(11):2619-2630